Journal of Materials & Environmental Sustainability Research (2025), 5(1): 1-14
p-ISSN: 2811-1338; e-ISSN: 2811-132X
DOI: https://doi.org/10.55455/jmesr.2025.001

Original Research Paper

Influence of the weaving method (plain, twill, satin) on the hydrodynamic behaviour of filtration membranes based on banana pseudostem fibres (Musa balbisiana)

NSOE Mengue JJ.N.[1, 2*], AMBA Esegni V.[1], Daniel E. EGBE.[1], BOUDINA J.M.[1], KAMENI Ngounou M.[1,4], KOFA Guillaume P.[1], NDI Koungou S.[1,3], KAYEM Guifo J[1].

1 Water Treatment and Filtration Research (Chem. Eng.) Group, Department of Process Engineering, ENSAI, University of Ngaoundere, P.O. Box 455, Ngaoundere, Cameroon
2 Laboratory of Chemical Engineering and Environment, University Institute of Technology (IUT), P.O. Box: 455 University of Ngaoundere, Cameroon
3 Department of Renewable Energies, University of Ebolowa, Cameroon
4 Research Center, National Advanced School of Public Works, P.O. Box 510, Yaounde, Cameroon

*Corresponding author: Nsoe Mengue N (nsoemenguenestor@yahoo.fr)

*Received: **February 15, 2025**; Received in revised form: **March 26, 2025**; Accepted: **March 29, 2025**; Published: April 21, 2025*

Abstract

The way in which a filtration membrane is woven influences its lifespan and purification performance. This study explores the impact of the weaving method on the hydrodynamic stability of a membrane made from banana pseudotrunk fibres. After extraction, the yarns were characterised. Three membranes were obtained using different weaving methods (plain, twill and satin), and the hydrodynamic study was used to determine the surface density, porosity, permeability and membrane resistance. Filtration tests were carried out on a suspension of 30 NTU, and the yarn obtained had a twist number of 10, a diameter of 0.75 mm and a tex of 168. The surface density and the percentage of surface voids for the three membranes, plain, twill and satin, were 8.82 g/m^2 and 50%, 12.54 g/m^2 and 30% and finally 15.77 g/m^2 and 12.54%. The uni membrane showed the best permeability, i.e. 5.60 x 10^{-10} m^2, but lower particle retention with a residual turbidity of 12 NTU, compared with the twill and satin membranes, which have permeability values of 5.31 x 10^{-10} m^2 and 4.80 x 10^{-10} m^2 and 9 and 7 NTU. The twill membrane appears to be the most suitable for filtration.

Keywords: Banana fibers; weaving; hydrodynamics; filtration

DOI: 10.55455/jmesr.2025.001

1. Introduction

Water Membranes separation processes play a crucial role in many separation applications ranging from waste water treatment to drinking water and the filtration of particles in food suspensions (Begum et al., 2021). These membranes are made from synthetic polymer materials of varying compositions. The diversity of their chemical compositions give them excellent properties (rigidity, flexibility or elasticity, mechanical and chemical resistance). This is why their annual production has risen from 1.5 million tonnes in 1950 to more than 350 million tonnes today and it is still growing steadily after use, synthetic polymers are released into the environment causing major environmental problems (Kozlowski et al., 2010; Sulastri and Rahimidar, 2016). At the end of their useful life, these filters are discarded in the natural environment. Ingestion of the fragments causes internal injuries or blocks digestion, increasing morbidity and mortality in living creatures. It is estimated worldwide, around half of all sea turtles have ingested these polymers, although the exact proportion is not known (Gregory, 2009). The small size of microplastics facilitates their passage through gastrointestinal membranes and their distribution in tissues and

organs resulting in the induction of oxidative stress, genome instability, disruption of the endocrine system, reproductive abnormalities, embryo toxicity and trans-generational toxicity (Alimba and Faggio, 2019; Wilcox et al., 2018). Nowadays, the widespread awareness of ecological and socio-economic imperatives, the search for sustainable green technologies, the growing problem of waste, environmental legislative standards and the depletion of fossil resources have led scientific research to focus on the development of membranes based on natural fibers (Wafiroh et al., 2021; Ortega, et al., 2014; Tserki et al., 2005). Natural membranes such as cotton, coconuts, flax and hemp offer many advantages in the field of water treatment. They are biodegradable, renewable and require less energy to produce (Rajendran et al., 2016). What's more, their molecular structure gives them a high affinity for certain pollutants such as heavy metals, oils and dyes (Baghel et al., 2020; Gao et al., 2019). But setting up a natural membrane requires prior study as with weaving. Several weaving modes influence the hydrodynamics and efficiency of a natural membrane depending on its nature (Mao, 2011; Behera and Hari, 2010; Espinasse et al., 2008; Bessière, 2005; Duroudier, 1999; Daufin et al., 1998). The weaving mode can be twill, satin or plain and the choice of a weaving mode will depend on the hydrodynamic behaviour and filtration performance of the membrane. Hence the interest of this work is to choose the best weave that gives the best hydrodynamic and filtration behaviour for woven membranes from banana pseudo-stem fibers.

2. Materials and Methods

2.1 Banana pseudo-stem

The banana pseudo-stem (**Figure 1**) used in this study comes from banana trees in a field in Ngaoundere (Cameroon) at coordinate points 7.422080 N and 13.544220 E (**Figure 2**). It is approximately 1m long, 30 cm in diameter and belongs to the Musaceae family.

Figure 1. Banana pseudo-stem

Figure 2. Harvesting field

2.2 Filtration pilot

In order to carry out this study, we set up a filtration test pilot. **Figure 3** shows the set-up of the filtration test pilot. The operation of this pilot starts with a stirring tank, where a pump draws the solution towards the filtration

module via a flow meter. A digital manometer is fitted to the filtration module to measure the transmembrane pressure (TMP).

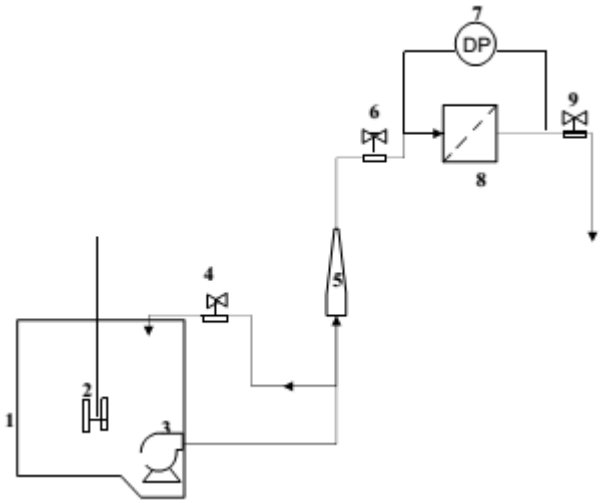

Figure 3. 1. Bach, 2. Agitator, 3. Pump, 4, 6, & 9. Valves, 5. Flowmeter, 7. Pressure gauge and 8. Filtration membrane.

2.3 Preparation of the concentration suspension

The laterite was sampled at Ngaoundere third in the locality of Gada Mbidou at the following geographical coordinates 7.4167420 North and 13.5547060 South according to the AFNOR NF P94-202 1995 standard and the preparation of the suspension was carried out according to the method of (Kameni et al., 2019).

2.4 Extraction of banana fibers

Banana fiber is extracted using the modified method of (Pratikhya et al., 2023). The aim is to obtain fibers of good length as shown in **Figure 4**.

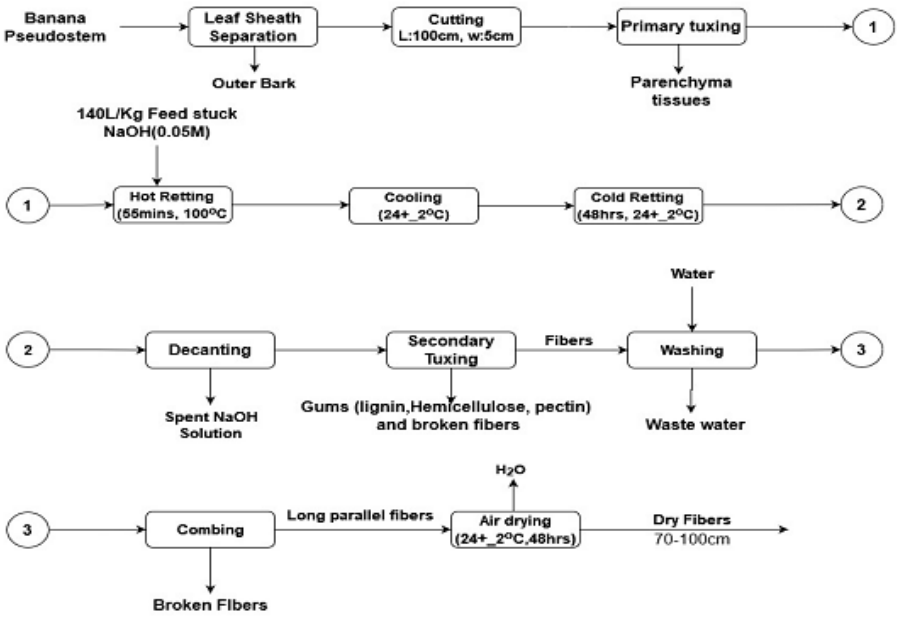

Figure 4. Banana fibre extraction process (Pratikhya et al., 2023).

2.5 Characterisation (density, cellulose content and breaking strength) of untreated and treated fibers

The cellulose content of the fibres was determined using the ISO 6865 method, density according to standard (NF T 51-003) and ASTM D570 was used to measure the absorbed water content (swelling test). The manual method of pulling fibers at different weights was used to obtain rapid measurements of breaking strength. Assuming that the woven fibers have a cylindrical geometry, we set a height of 3.5 cm and a diameter of 1 mm.

2.6 Banana fiber yarn production and characterisation

The spinning operation was carried out in the "S" direction (clockwise), on a number of 10 turns, the diameter of the yarn over its entire length was monitored using the calliper in order to produce yarns with uniform diameters.

2.6.1 Fineness

Fineness is one of the characteristics of fibres and is measured in tex. A unit of linear mass equal to 1 gram of fiber per kilometre of length. This expression can also be used to evaluate the fineness of the fibre or yarn in tex (Sutherland and Purchas, 2000).

$$\text{Tex} = \frac{590{,}6.\text{W.l}}{\text{L.w}} \qquad (1)$$

Where, W is the Fiber mass, L is the fiber length, l is the unit of sample length (840 yards or 768.096 m) and w is the unit of mass of the sample (453.6 g).

2.6.2 Porosity

The porosity of the yarn (Eq. 3) depends on the number of spinning operations carried out during the manufacture of the yarn, as well as the diameter of the yarn. This influences the pressure and therefore reduces the filtration efficiency (Kanade, 2023, Venkataravanappa et al., 2023). Considering the density of the fibre which is 1.03 g/cm^3 (Abdul et al., 2019). The value of fiber packing (ϕ) is given by the expression of (Turan et al., 2013). This value of ϕ is calculated using Eq. 2.

$$(\emptyset) = \frac{[3.37*10^{-3}*\sqrt{\text{tex}}]\text{^}2}{[\text{D}*\sqrt{\rho s}]\text{^}2} \qquad (2)$$

The value of packing and porosity are inversely related such that, a high value of packing leads to low porosity and can therefore be given by the following expression:

$$\text{Porosity} = 1-\emptyset \qquad (3)$$

2.7 Manufacture and characterisation of the membrane

In order to produce a flat filter element, a weaving loom (**Figure 5A**) was used. This loom has 3 zones allowing the desired surfaces to be produced, a smaller zone (792 cm^2), a medium zone (3480 cm^2) and a larger zone of 4800 cm^2. The loom was then armed with banana fibre yarns (**Figure 5B**) as warp and weft yarns in order to produce plain, twill and satin weaves (**Figure 5C**).

2.7.1 Surface density of the membrane

The surface density of a membrane refers to the number of threads used in the design of a fabric per unit area. In filtration, the density of a woven filter element is a characteristic that can influence its permeability and is a factor to be taken into consideration when choosing a filter element. Its expression (equation 4) according to (Hanafi et al., 2013) is as follows:

$$\text{D}_s(\text{g/m}^2) = \frac{\text{Masse of filter media}}{\text{Filter media surface area}} \qquad (4)$$

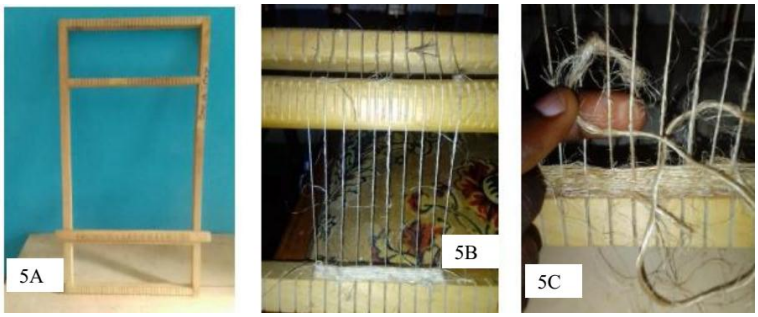

Figure 5. Stages in the production of woven membranes from banana pseudo-stem fibres (loom (5A), warp, weft yarn (5B) and weaving (5C).

2.7.2 Membrane porosity

Where D_s the surface mass of the membrane (gm^{-2}), e its thickness (m) and ρ_f the density of the fibers (gm^{-3}). The expression for the porosity of the membrane according to (Begum et al., 2021) is as follows:

$$\varepsilon = 1 - \frac{Ds}{e.\rho_f} \quad (5)$$

2.7.3 Experimental determination of membrane permeability and resistance

These tests were carried out using osmosis water, as this is free from clogging materials. When the system was set up, the membrane was immersed in the distilled water contained in the housing. After running the system for 1 hour, increasing filtration flows were imposed and the transmembrane pressure (TMP) was measured using an electronic manometer (KELLER MANNO 200 Model LEO 2, USA). Knowing the physico-chemical properties of the water (in particular the viscosity at the temperature of the test bath), the application of Darcy's generalised law in a filtering medium (Eq. 6) enabled us to determine the membrane permeability. The specific resistance R is simply deduced from the equation (Eq. 7) and is the inverse of the permeability. Its expression is represented by equation (Eq. 8).

$$J = \frac{\boldsymbol{TMP}}{\boldsymbol{\eta R}} \quad (6)$$

$$J = \frac{Q_f}{\boldsymbol{S}} \quad (7)$$

$$R = \frac{\mathbf{1}}{\boldsymbol{\eta Lp}} \quad (8)$$

Where J: Permeate flux ($m^3.m^{-2}.s^{-1}$), Q_f: Permeate flow rate ($m^3.s^{-1}$), Lp: Membrane permeability to solvent (m^{-2}), S: Membrane surface area (m^2), TMP: Transmembrane pressure (Pa), n: Permeate viscosity (Pa s), R: Membrane resistance (m^{-1}).

2.8 Conducting pilot tests

These tests were conducted with a 300 NTU suspension at a constant pressure of 0.1 bars and in a laminar flow regime. The permeability values for the different membranes were calculated using Darcy's equation (Nsoe et al., 2023, Begum et al., 2021).

$$Q = \frac{\beta.(-\Delta P)}{\mu_f.e} \quad (9)$$

Where β the coefficient of permeability in m^2, ΔP the pressure drop in Pa, Q the volume flow rate in $Lmin^{-1}$, μf the dynamic viscosity of the fluid in Pa.s, e the membrane thickness in m.

2.9 Particle size distribution of sludge (Cut-off threshold)

The particle size distribution in water was determined using a MASTERSIZER (HYDRO 2000SM) laser granulometer from MALVERN Instruments (UK). It is used to obtain the particle size distribution of a sample (<100 µm) in the form of a frequency curve. All particles illuminated by a laser beam diffract light in all directions with an intensity distribution that depends on their size.

2.10 Clogging power evaluation parameter

The resistance αC and the specific resistance α were calculated from the experimental data and Eq. 10 (Contreras et al., 2009).

$$\frac{t}{V} = \frac{\mu}{S.\Delta P} * \left(\alpha \frac{CV}{2.S} + R_m\right) \quad (10)$$

Where t is the time in s, V is the volume filtered m^3, S is the membrane surface area in m^2, α is the specific resistance of the deposit in mkg^{-1} and C is the membrane concentration in kgm^{-3}.

3. Results and discussion

3.1 Fibers characteristics

Table 1. Fibers characteristics

Characteristics	
Extraction yield (%)	5.90
Water content (%)	17.76
Fiber length (cm)	85.45
Swelling (%)	81.51

Table 1 shows that the water content is 17.76 %, which is higher than the values found by Marie (2021), Mbouyap et al., (2020) and Athijayamani et al., (2010), who obtained a water content of 10-11% with an average length of 2 cm. The length of the fibers obtained was 85.45 cm. This difference can be explained by the extraction procedure. Mbouyap et al., (2020) used biological extraction, while Abdul et al., (2019) used soda extraction followed by sun drying. Here, the fibers were stored in an air chamber. This results in a relatively high water content. According to Pratikhya et al., (2023), fibers that are too dry lead to breakage and fibre loss during combing. It should be noted that the higher the moisture content of the fibre, the higher the pith content and the more likely it is to be attacked by bacteria (Lerch, 2015, Kozlowski et al., 2010). For this reason, the process modified by Pratikhya et al., (2023) proved to be the most suitable for producing fibres suitable for the production of woven filter media. The swelling test was 81.51% demonstrating the hydrophilic nature of banana fiber, a feature sought after by most filter media designers in order to minimise the resistance to the passage of water through the filter media which is greater when the fiber is hydrophobic.

3.2 Wire characteristics

Table 2 shows that the yarn has a length of 0.75 mm in diameter, the maximum torsion supported by the fibres is 10, beyond which the yarn breaks and the yarn obtained at the end of the process has a fineness of 168 tex with a porosity of 0.5. These values are typical of the yarns used to manufacture natural membranes. This confirms the importance of the extraction method. In fact, this technology is used in the production of smooth filaments

creating, an effective porous yarn for deep retention and microfiltration membranes (Pratikhya et al., 2023; Marie, 2021; Lerch, 2015).

Table 2. Characteristics of the wire produced

Characteristics	
Types	S
Number of twists	10
Tex	168
Wire diameter (mm)	0.75
Porosity	0.5

3.3 Characteristics of the filter media

Three basic types of weave were used (plain, twill and satin). **Table 3** shows the characteristics of these membranes after production. The table shows that characteristics such as mass, number of warp interlacings and surface density of the media are a function of the different types of weave. The difference between the plain-twill media is 2.63 gm^{-2} and that between the twill-satin media is 2.28 gm^{-2}. From these observations, it follows that the twill weave in terms of retention is closer to the satin media, whereas the difference in porosity between the plain-twill membranes is 0.14, and the difference between the twill-satin membrane is 0.08. From this observation, we can conclude that there is not a very significant difference in porosity between the twill and satin membranes (Lerch, 2015). Compared to filter media used in filtration such as polypropylene, these different types of weave offer very good efficiency (Kanade, 2023). However, the specific filtration efficiency depends on the material such as banana pseudo-stem fibers which have a larger diameter which results to larger pore sizes, compared with polypropylene fibers whose diameter can be controlled during the manufacturing process, such as weaving and calendering, to produce effective membranes, particularly for capturing smaller particles (Sumesh et al., 2022).

Table 3. Characteristics of the filter media manufactured

Types of media	Mass (g)	Number of Chain interleaves	Number of interleaves Frame	Surface density of media (g/m^2)	Porosity
Plain	5.87	110	10	8.82	0.5
Twill	8.34	200	10	12.54	0.3
Satin	10.49	287	10	15.77	0.18

Figure 6 shows that the plain, twill and white satin weaves give us permeabilities of 5.60 x 10^{-10} m^2, 5.31 x 10^{-10}, and 4.81 x 10^{-10} m^2. By evaluating the standard deviation of permeability between the membranes, we can see that there is a difference of 2.05 x 10^{-11} m^2 for the plain and twill weave, and 3.53 x 10^{-11} m^2 for the twill and satin weave. We can therefore deduce that the twill weave gives us a membrane with a permeability of 2.05 x 10^{-11} m^2 close to that of the plain membrane. This result is in line with the findings of Mao, (2011), who studied the permeation rate of water through woven membranes and concluded that the type of weave influences the thickness of the membrane, which in turn has an effect on the permeation rate of the membrane. By observing the difference in porosity, the twill membrane is closer to the satin membrane and we can conclude from this observation that this type of weave allows for tighter meshes and gives the hydrophilic nature of the fibres. This facilitates the flow of fluid within the membrane with a resistance value of 1.8 x 10^9 m^{-2}. **Figure 7** on the other hand, shows the histogram of flow resistance as a function of weave type. It can be seen from this histogram that the type of weave

affects resistance and the weave with the greatest resistance is the satin type. This can be explained by the fact that interweaving the threads by overlapping them makes the latter denser, which increases resistance to the passage of water through the membrane. This difference can also be explained by the thickness of the woven membranes (Jermann et al., 2008).

3.4 Membrane permeability and resistance

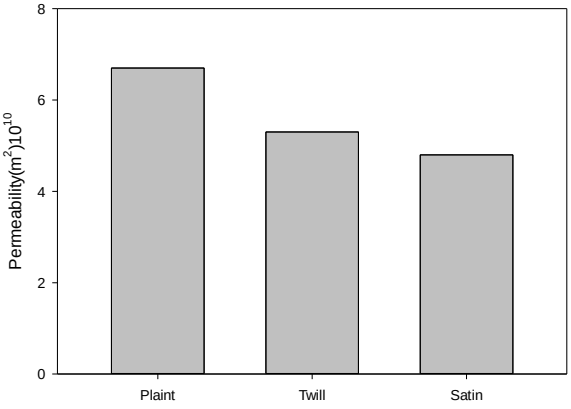

Figure 6. Permeability as a function of weave type

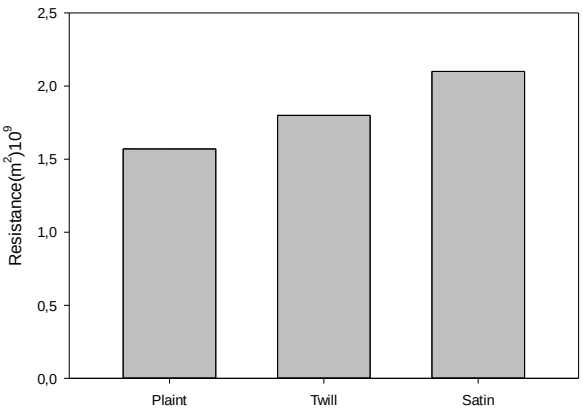

Figure 7. Influence of weaving method on strength

3.5 Evaluation of the flow generated as a function of the pressure drop

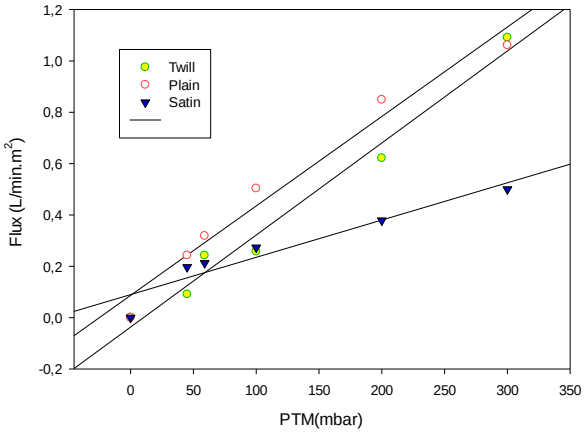

Figure 8. Variation in flux as a function of TMP with different types of membrane in distilled water

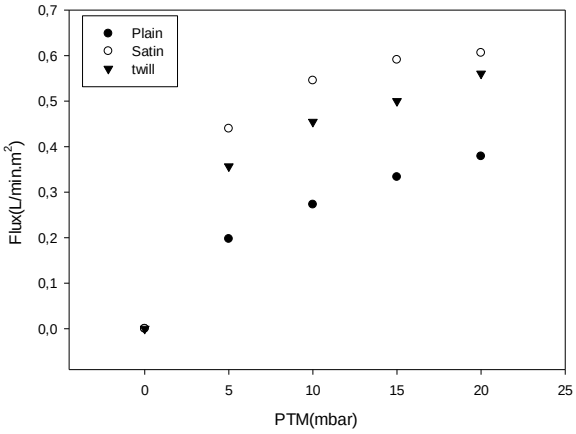

Figure 9. Flux variation as a function of TMP with different types of membrane in a lateritic solution

The curves in **Figures 8** and **9** show an increase in flux whatever the membrane and operating conditions. However, in **Figure 8** this evolution is linear showing that our curves obey Darcy's law (Sutherland and Purchas, 2000). The blank transmembrane pressure (TMP) as a function of the flow generated for each of the filter media shows for a maximum value of TMP (300 mbar), flow values of 0.75 $Lmin^{-1}$ for the unit membrane, 0.59 $Lmin^{-1}$ for the twill membrane and 0.33 $Lmin^{-1}$ for the satin membrane. The observed flux values can be explained by the resistance and permeability histograms presented above, given the manufacturing variability, the low flux obtained by satin weave is due to the high resistance observed in **Figure 6**. For the membranes obtained by twill and plain weaves, the maximum value of linear flux generated is much higher than the flux obtained by the satin membrane. This can be explained by the fact that satin weave makes it possible to obtain membranes with a low porosity (0.18) as shown in **Table 3**. On the other hand, in **Figure 9**, under filtration test conditions, the flux does not follow Darcy's law. The drop in flux as a function of the type of weave is proportionally linked to the porosity values of the membranes due to the fact that the particles in suspension have more or less the size of the pores in each membrane. It should also be noted that the less porous the filter media, the greater the speed at which the

cake is formed, which is observed in the case of satin-finish membranes. In conclusion, PTM is caused by the combination of two resistances to flow present under operating conditions such as the resistance of the membrane and that of the cake formed.

3.6 Effect of weaving method on turbidity

Figure 10 shows the variation in turbidity as a function of the type of woven media. These observations show that for the three types of membrane, turbidity decreases as a function of time from an initial value of 30 NTU to final values of 12 NTU for plain weaves, 9 NTU for the twill membrane and 7 NTU for the satin membrane. 70.33% turbidity abatement for the plain media, 82.33% for the twill media and 84.33% for the satin media. By grouping together the graphs showing the effect of the weaving method on turbidity and the graph showing the change in head loss as a function of time for the 3 weaving methods. It can be seen that a reduction of 70.33% for plain weaving over 15 hours of operation generates a head loss of 144 mbar and a pressure drop of 144 mbar. For an abatement of 82.33% for the twill weave, the pressure drop generated is 171 mbar and for an abatement of 84.33% the pressure drop for the twill weave is 198 mbar. The difference between the plain-twill media is 12% abatement and 27 mbar pressure drop difference. For the twill-satin weaves the abatement difference is 14% and 54 mbar pressure drop difference. Finally, for the uni-satin weave, the abatement difference is 2% with a pressure drop difference of 27 mbar. The most likely media for use in filtration is twill media. The above information shows the advantages of using these membranes. Turbidity reduction by these membranes is directly linked to their porosity which is 0.5, 0.3 and 0.18 for plain, twill and satin membranes respectively. The head loss behaviour is a function of the total flow resistance of each membrane.

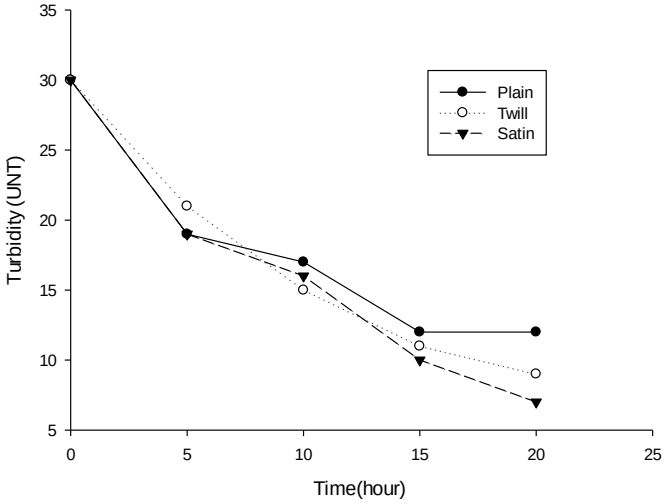

Figure 10. Turbidity variation as a function of time at different weaving modes (plain, twill, satin).

3.7 Cut-off threshold for different membranes

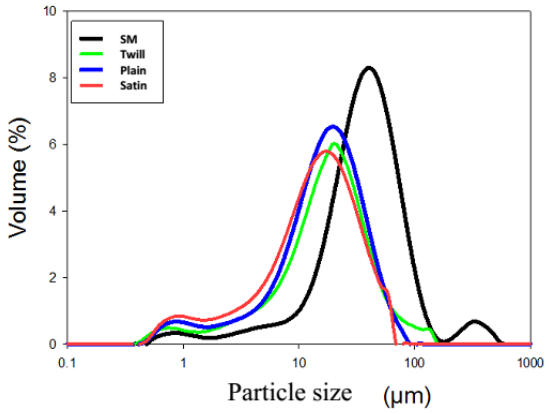

Figure 11. Particle size distribution as a function of weave type.

In order to determine the cut-off for the different membranes, a particle size analysis was carried out. **Figure 11** shows the particle size distribution before and after filtration for different membranes. The above figure confirms the results obtained earlier. The cut-off threshold varies according to the type of weave. For the plain weave, with 50% void space, the diameter of the particles likely to pass through the membrane is 29 µm for the serge membrane, 30% void space allows the passage of particles of 21 µm, and finally for the satin membrane 18% void space allows particles of 15 µm diameter to pass through the membrane. The particle size distribution of the mother solution is composed of two families of particles, so it is reasonable that depending on the diameter of each membrane, the larger particles will accumulate on the surface of the different membranes and form a filter cake that will negatively affect the flow (Kanade, 2023). In view of the hydrodynamic characteristics obtained, the best type of weave for a more economical filtration process is twill weave.

3.8 Effect of the weaving method on the clogging mechanism

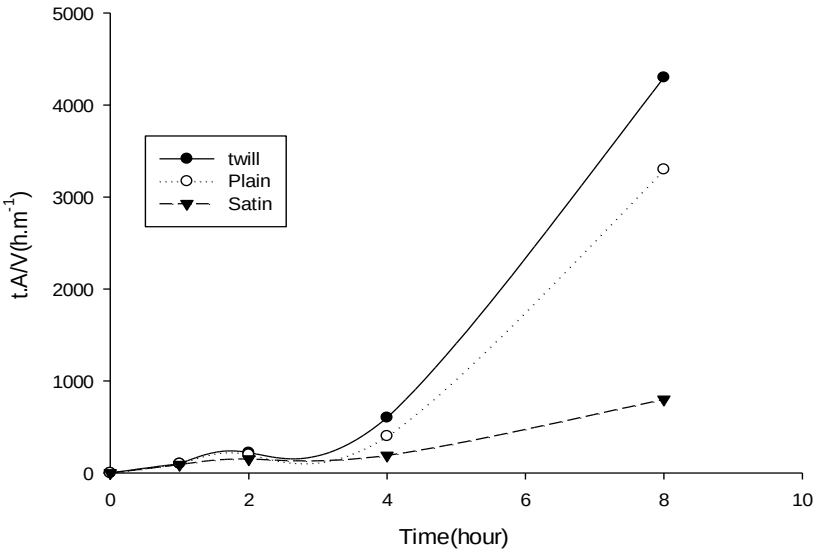

Figure 12. Clogging mechanisms as a function of time for different types of weave.

Figure 12 shows that at the start of filtration, between 0 and 2 hours, there is little clogging. After this time, we see a linear increase in clogging for the serged and satin-finish membranes, while for the plain membrane it tends to remain constant after 3 hours of filtration. From 4 to 8 hours, there is a sudden increase in clogging. This phenomenon can be explained by the fact that at the start of filtration, the membranes are still clean and unclogged, which gives us low clogging values. This is due to the maximum availability of the membrane pores to allow the fluid to pass through (Sutherland and Purchas, 2000). However, as filtration time elapses, clogging increases, leading to obstruction of the membrane pores which reduces the effective surface area available for filtration and increases resistance to the passage of fluid through the membrane, resulting in increased clogging (Contreras et al., 2009).

3.9 Characteristics of membranes after filtration

Table 4. Summary table of filter media characteristics

Types of weave	Thickness of filter element (s)(m)	Porosity (ε)	Effective resistance of the filter element (Rm)(m^{-2})	Cake resistance (Rg)(m^{-2})	Compressibility index	Cake mass (W)gm^{-2}
Plain	0.001	0.5	2.57×10^{9}	1.76×10^{11}	0.81	26.34
Twill	0.004	0.3	2.76×10^{9}	3.01×10^{11}	1.0	35.11
Satin	0.006	0.18	2.86×10^{9}	3.38×10^{11}	1.1	43.23

Table 4 shows the characteristics of the different membranes after filtration tests. For the membrane obtained by plain weave, the total effective resistance is 1.78×10^{11} m^{-2}, for the twill membrane the total resistance is 3.03×10^{11}

m^{-2} and for the satin membrane the total resistance is 3.41x 10^{11} m^{-2}. According to this table, these resistances are proportional to the mass of the cake formed on the membrane surface. During filtration, the progressive accumulation of cake induces resistance at the membrane, which progressively affects the output flow. This table also shows the compressibility index which indicates that the membrane compresses more under pressure during filtration. This may be due to the nature of the material, as well as the porous structure of the material. For the different membranes, the indices range from 0.81 for the plain membrane, 1.0 for the twill membrane and 1.1 for the satin membrane. These differences are due to the influence of the porosity of each membrane, which has an influence on the transmembrane pressure.

3.10 Influence of weaving type on flow during filtration

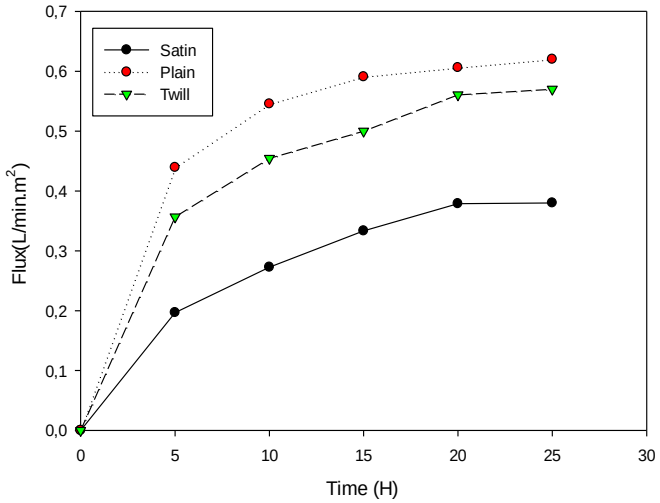

Figure 13. Variation of flux as a function of time during filtration of a 30 NTU suspension for different membranes.

The shape of these curves confirms the information on the clogging mechanism showing that, for the different membranes the flux increases linearly up to a value of 0.20 L/min.m² for the satin membrane, 0.44 L/min.m² for the twill membrane and 0.47 for the membrane obtained using the uni membrane. For the membranes obtained by twill and plain weaves, the maximum value of linear flux generated is much higher than the flux obtained by the satin membrane. This can be explained by the fact that the satin weave makes it possible to obtain membranes with a low porosity (0.18), this is why during the filtration of turbidity suspensions (30 NTU), there is rapid formation of the filter cake. By observing the nominal filtration values for each membrane, it is possible to estimate the time required to form the first layer of cake which is 2hour 25 min for the plain membranes, 1hour 45 min for the twill membrane and 1hour 35 min for the satin membrane.

4. Conclusion

Throughout our study, the impact of the weaving method on filtration hydrodynamics was evaluated. Therefore, three types of conventional weave such as plain, twill and satin weaves were performed. The technique used for the design of each membrane affects the weave density and porosity. The filtration tests revealed that, the satin weave presents the highest resistance to flow, with a low permeability value and a high pressure drop compared to the plain and twill membrane, but this membrane presents a better retention. The membrane with the lowest turbidity value is the plain weave membrane. From an overall point of view, it can be seen that an increase in weave density leads to a decrease in permeability which increases resistance to flow. Comparing these three membranes, the twill membrane appears to be the most suitable for filtration.

Funding: No financial support was received.

Declarations

Conflict of interest: The authors declare that they have no conflict of interest.

Data Availability: The authors declare that the data supporting the findings of this study are available within the paper

Ethical Approval: This article does not contain any studies with human participants or animals performed by any of the authors.

Informed Consent: None.

Research Involving Human and Animal Rights: This article does not contain any studies involving animals or human participants performed by any of the authors

References

Abdul, C. S., Ganemulle, L. D. and Ujithe, S.W. (2019). Effect of physical, chemical and biological extraction methods on the physical behaviour of banana pseudo-stem fibres: Based on fibres extracted from five common Sri Lankan cultivars. *Journal of Engineered Fibers and Fabrics*., 14:12-25

Alimba, C. G. and Faggio, C. (2019). Microplastics in the marine environment: Current trends in environmental pollution and mechanisms of toxicological profile. *Environ. Toxicol. Pharmacol*., 68, 1-164

Athijayamani, A., Thiruchitrambalam, M., Natarajan, U. and Pazhanivel, B. (2010). Influence of alkalitreated fibers on the mechanical properties and machinability of roselle and sisal fiber hybrid polyester composite. *Polymer Composites*., 31:723–31

Baghel, S., Poornima, S., Tejal, K., Sourish, B. and Annamma, A. (2020). Seaweed biorefinery: A sustainable process for valorising the biomass of brown seaweed. *Journal of Cleaner Production*., 263(21):121359.

Begum, M. T., René I., Peinadord, J, I., Calvo, A. H. and JiaWei, C. (2021). Porosimetric membrane characterization techniques: a review. *Journal of Membrane Science.,* 619(3): 118750

Behera, B. K. and Hari, P. K. (2010). Woven textile structure: Theory and applications.

Bessière, Y. (2005). Filtration frontale sur membrane : mise en évidence du volume filtré critique pour l'anticipation et le contrôle du colmatage. Université Paul Sabatier.

Contreras, A. E., Kim, A. and Li, Q. (2009). Combined fouling of nanofiltration membranes: Mechanisms and effect of organic matter. *Journal of Membrane Science.,* 327, 87–95

Daufin, G., René, F. and Aimar, P. (1998). Les séparations par membrane dans les procédés de l'industrie alimentaire.

Duroudier, J. P. (1999). Les supports filtrants, in Pratique de la filtration, HERMES Science Publications: Paris.

Espinasse, B., Bacchin, P. and Aimar, P. (2008). Filtration method characterizing the reversibility of colloidal fouling layers at a membrane surface: Analysis through critical flux and osmotic pressure. *J. Colloid Interface Sci*., 320, 483–490

Gao, J., An, Z. and Bai, X. (2019). A new representation method for probability distributions of multimodal and irregular data based on uniform mixture model. *Annals of Operations Research*. 19:32-46

Gregory, M. R. (2009). Environmental implications of plastic debris in marine settings entanglement, ingestion, smothering, hangers-on, hitch-hiking and alien invasions. Philosophical Transactions of the Royal Society B: *Biological Sciences*., 364. 2013-2025

Hanafi, Y., Baddari, K., Szymczyk, A. and Zibouche, F. (2013). Caractérisation de la densité de charge de surface de membranes nanoporeuses. *Journal of Materials, Processes and Environment*., 1:211-223

Jermann, D., Pronk, W., Kägi, R., Halbeisen, M. and Boller, M. (2008). Influence of interactions between NOM and particles on UF fouling mechanisms. *Water Research.*, 42, 3870–3878

Kameni, N. M., Ndi, K. S., Kofa. G. P. and Kayem, G. J. (2019). Coagulation and sedimentation of concentrated laterite sus- pensions: comparison of hydrolysing salts in presence of Grewia spp. biopolymer, *Journal of Chemistry*., 9, ID 1431694, 9

Kanade, P. (2023). Role of Spinning Machine Process Variables on Porosity of DREF Spun Yarn. *Fibers Polym.,* 24, 2521–2527

Kozlowski, R. M., Mackiewicz-Talarczyk, M. and Barriga-Bedoya. J. (2010). "Natural Fibers Production, Processing, and Application: Inventory and Future Prospects," in Contemporary Science of Polymeric Materials. *American Chemical Society*., 1061, 3–4

Lerch, T. P. (2015). Determination of surface density of nonporous membranes with air-coupled ultrasound. *AIP Conf. Proc.*, (1): 1292–1298

Mao, C. D. (2011). Effect of fabric construction on water permeability rate of woven filter cloth. *Advanced material Research*, 331, 48-51

Marie, G. (2021). Extraction des fibres de chanvre pour des composites structuraux – Optimisation du potentiel mécanique des fibres pour des applications concernant des matériaux composites 100% bio-sourcés. Matériaux et structures en mécanique [physics.class-ph]. Institut National Polytechniquede Toulouse - INPT, 2021. Français. NNT: 2021INPT0002ff. tel-04165247ff

Mbouyap, C. T., Tchotang, C., Bopda, F. and Kenmeugne, B. (2020). Influence of extractions techniques on the physico-mechanical properties of banana pseudo- stem fibers., *J. Mater. Environ*. Sci. 11(7), 1121-1128

Nsoe, M. N., Amba, E.V., Kameni, N.M., Kofa, G.P., Ndi, K.S., Heran, M. and Kayem, G.J. (2023). Biodegradation of Natural Rubber Wastewater in the Submerged Membrane Bioreactor by Pichia Guilliermondii and Yarrowia Lipolytica. *International Journal of Membrane Science and Technology*., 2023, 10, 38-46

Ortega, E., Martín, B., Nuñez, A. and Ezquerra, A. (2015) Urban Fragmentation Map of the Chamberí District in Madrid. *Journal of Maps*, 11: 788-797.

Pratikhya, B., Seiko, J. and Gautam, B. (2023). Banana pseudo stem fiber: A critical review on fiber extraction, characterization, and surface modification, *Journal of Natural Fibers.*, 20:1-12

Rajendran, K.V., Shivam, S., Ezhil, P., Sahaya R. and Sathish Kumar, T. (2016). Emergence of Enterocytozoon hepatopenaei (EHP) in farmed Penaeus (Litopenaeus) vannamei in India., *Aquaculture*, doi: 10.1016/j.aquaculture.2015.12.034

Sulastri, A. and Rahimidar, L. (2016). Fabrication de biomembrane à partir de tige de banane pour l'élimination du plomb. *Journal Indonésien des Sciences et Technologies*., 1(1): 115 - 131

Sumesh, K. R., Kavimani, G., Rajeshkumar, S. I. and Khan, A. (2022). Mechanical, water absorption and wear characteristics of novel polymeric composites: Impact of hybrid natural fibers and oil cake filler addition. *Journal of Industrial Textiles*., 51 (4): 5910S–37

Sutherland, K. and Purchas D. (Eds.) (2002). Handbook of filter media. Elsevier

Tserki, V., Zafeiropoulos, N.E., Simon, F. and Panayiotou, C. (2005). A study of the effect of acetylation and propionylation surface treatments on natural fibres. Composites Part A: *Applied Science and Manufacturing*., 36(8), 1110-1118

Turan, R., Befru, O. and Ayse, I. (2013). "Prediction of the in-plane et through-plane fluid flow behavior of woven fabrics." *Textile Research J., 5*: 700-717.

Venkataravanappa, R.Y., Lakshmikanthan, A., Kapilan, N., Chandrashekarappa, M.P.G., Der, O. and Ercetin, A. (2023). Physico-Mechanical Property Evaluation and Morphology Study of Moisture-Treated Hemp–Banana Natural-Fiber- Reinforced Green Composites. *J. Compos. Sci.,* 7, 266

Wafiroh, S., Abdulloh, A. and Widati, A. (2021). Fibres creuses d'acétate de cellulose revêtues de Ti_2O pour la dégradation des déchets de teinture textile. *Technologie chimique.* 15 (2): 291 -298.

Wilcox, C., Puckridge, M. and Schuyler, Q. A. (2018). A quantitative analysis linking sea turtle mortality and plastic debris ingestion. *Sci Rep.,* 8: 12-26